THE JOURNAL OF BIOLOGICAL CHEMISTRY VOL. 285, NO. 33, pp. 25645–25653, August 13, 2010

Store-operated Ca^{2+} Entry in Malignant Hyperthermia-susceptible Human Skeletal Muscle*[S]

Received for publication, January 17, 2010, and in revised form, June 18, 2010 Published, JBC Papers in Press, June 21, 2010, DOI 10.1074/jbc.M110.104976

Adrian M. Duke[‡], Philip M. Hopkins[§], Sarah C. Calaghan[‡], Jane P. Halsall[§], and Derek S. Steele[‡1]

From the [‡]Institute of Membrane and Systems Biology, University of Leeds, Leeds LS29JT and the [§]Leeds Institute of Molecular Medicine, St. James's University Hospital, Leeds LS9 7TF, United Kingdom

In malignant hyperthermia (MH), mutations in RyR1 underlie direct activation of the channel by volatile anesthetics, leading to muscle contracture and a life-threatening increase in core body temperature. The aim of the present study was to establish whether the associated depletion of sarcoplasmic reticulum (SR) Ca^{2+} triggers sarcolemmal Ca^{2+} influx via store-operated Ca^{2+} entry (SOCE). Samples of vastus medialis muscle were obtained from patients undergoing assessment for MH susceptibility using the *in vitro* contracture test. Single fibers were mechanically skinned, and confocal microscopy was used to detect changes in $[Ca^{2+}]$ either within the resealed t-system ($[Ca^{2+}]_{t\text{-}sys}$) or within the cytosol. In normal fibers, halothane (0.5 mM) failed to initiate SR Ca^{2+} release or $Ca^{2+}{}_{t\text{-}sys}$ depletion. However, in MH-susceptible (MHS) fibers, halothane induced both SR Ca^{2+} release and $Ca^{2+}{}_{t\text{-}sys}$ depletion, consistent with SOCE. In some MHS fibers, halothane-induced SR Ca^{2+} release took the form of a propagated wave, which was temporally coupled to a wave of $Ca^{2+}{}_{t\text{-}sys}$ depletion. SOCE was potently inhibited by "extracellular" application of a STIM1 antibody trapped within the t-system but not when the antibody was denatured by heating. In conclusion, (i) in human MHS muscle, SR Ca^{2+} depletion induced by a level of volatile anesthetic within the clinical range is sufficient to induce SOCE, which is tightly coupled to SR Ca^{2+} release; (ii) sarcolemmal STIM1 has an important role in regulating SOCE; and (iii) sustained SOCE from an effectively infinite extracellular Ca^{2+} pool may contribute to the maintained rise in cytosolic $[Ca^{2+}]$ that underlies MH.

Although recent studies have demonstrated the presence of store-operated Ca^{2+} entry (SOCE)[2] in skeletal muscle (1, 2), the role of this Ca^{2+} influx mechanism remains uncertain. SOCE has typically been studied using protocols that involve caffeine-induced activation of RyR1 and/or inhibition of sarcoplasmic reticulum Ca^{2+}-ATPase to induce a profound depletion of sarcoplasmic reticulum (SR) Ca^{2+} (1–3). However, under physiological conditions, the amount of Ca^{2+} released during a tetanic contraction is typically <10% of the total SR Ca^{2+} content (4, 5) and apparently insufficient to activate SOCE (2, 6). This suggests that SOCE is unlikely to have a significant role in Ca^{2+} homeostasis during exercise of moderate intensity. SOCE might, however, be activated during intensive exercise leading to fatigue (7), where SR luminal Ca^{2+} declines (8, 9). Consistent with this possibility, a reduced capacity for SOCE has been linked to impaired fatigue resistance in aged murine skeletal muscle (10).

Another possibility not yet considered is that SOCE might contribute to the pathological rise in cytosolic $[Ca^{2+}]$ that underlies human malignant hyperthermia (MH). In most cases of MH, susceptibility is conferred by mutations in the gene encoding RyR1 (*RYR1*, chromosome 19q13.1) (11, 12). During an MH episode, activation of RyR1 by a volatile anesthetic induces SR Ca^{2+} release, muscle contracture, and a potentially fatal rise in core body temperature. Given this established sequence of events, it is generally assumed that the rise in cytoplasmic $[Ca^{2+}]$ during MH solely reflects Ca^{2+} efflux from the SR. However, activation of RyR1 and consequent depletion of SR Ca^{2+} might also induce SOCE, thereby triggering a sustained Ca^{2+} influx from an effectively infinite extracellular pool.

Interestingly, the involvement of extracellular Ca^{2+} in MH is suggested by findings that the anesthetic-induced contracture during the *in vitro* contracture test (IVCT) is markedly reduced in solutions lacking extracellular Ca^{2+} (13, 14). However, this observation is inconclusive because reduced binding of extracellular Ca^{2+} to the dihydropyridine receptor has been shown to inhibit pharmacological activation of RyR1 independently from Ca^{2+} entry (15), and thus the role of SOCE in human MH remains uncertain.

The aim of the present study was to establish whether SOCE is activated by volatile anesthetic exposure in human MH-susceptible (MHS) skeletal muscle. Experiments were done on normal (MHN) or MHS vastus medialis muscle obtained from patients undergoing MH diagnosis. Fibers were mechanically skinned, and confocal microscopy was used to detect changes in $[Ca^{2+}]$ within the sealed t-system or within the cytosol, using fluo-5N or fluo-3, respectively. The data provide the first evidence of SOCE in adult human skeletal muscle and show that clinically relevant levels of volatile anesthetic can induce Ca^{2+} influx, secondary to a submaximal SR Ca^{2+} depletion in MHS but not in MHN fibers. The characteristics of SOCE in human skeletal muscle and the possible involvement of sarcolemmal STIM1 in the Ca^{2+} influx mechanism are addressed.

* This work was supported in part by a grant from the Medical Research Council.

[S] The on-line version of this article (available at http://www.jbc.org) contains supplemental Figs. 1–3, Tables 1 and 2, and references.

[1] To whom correspondence should be addressed. Tel.: 44-1133432912; E-mail: d.steele@leeds.ac.uk.

[2] The abbreviations used are: SOCE, store-operated Ca^{2+} entry; MH, malignant hyperthermia; MHN, MH normal; MHS, MH-susceptible; SR, sarcoplasmic reticulum; ECCE, excitation-coupled Ca^{2+} entry; APACC, action potential-activated Ca^{2+} current; IVCT, *in vitro* contracture test; DMSO, dimethyl sulfoxide; HDTA, hexamethylenediamine-tetraacetate; STIM1 stromal interaction molecule 1.

EXPERIMENTAL PROCEDURES

Skinned Fibers—Samples of vastus medialis muscle were obtained by open biopsy from patients attending for MH diagnosis at St. James's University Hospital, Leeds, UK. Approximately 1 g of muscle was removed for use in the IVCT. With institutional Research Ethics Committee approval and informed patient consent, an additional bundle (0.2 g) was taken to provide material for mechanically skinned muscle experiments. All procedures were done according to the Declaration of Helsinki. The IVCT provided the primary method of categorizing tissue as MHN or MHS, according to the criteria for MH research of the European MH Group (16). This ensures a high sensitivity and specificity of the MHS diagnosis (98 and 94% respectively)(17).

With institutional review board approval, all patients consented to provide a blood sample for DNA analysis. DNA was extracted from whole blood, and RYR1 mutation analysis was conducted (18). The MHS samples used in this study originated from 13 patients (supplemental Table 1). 11 of the samples were from patients with one of 34 recurrent RYR1 mutations (supplemental Table 2). The mutations were distributed among three hot spot regions (see the legend of supplemental Table 1 for details).

Muscle samples were placed in paraffin oil to displace the extracellular fluid before isolation and mechanical skinning of individual fibers with fine forceps. Skinned fibers were suspended in a bath with an "internal" solution designed to mimic the intracellular environment (see below). Vastus medialis is of mixed fiber type, and Sr^{2+} sensitivity was used to classify the fibers as type 1 or type 2 (19). Most preparations did not generate tension at negative logarithm (base 10) of the molar concentration of Sr^{2+} 5.2, confirming that most fibers selected for skinning were type-2. Preparations generating tension at negative logarithm (base 10) of the molar concentration of Sr^{2+} 5.2 were excluded from the study.

Solutions—Unless otherwise stated, all chemicals were purchased from Sigma-Aldrich (Poole, UK). A basic internal solution was prepared comprising (in mM): 50 HDTA; 8 ATP; 37 Na^+; 126 K^+; 10 phosphocreatine; 0.1 EGTA; 90 HEPES. The free $[Mg^{2+}]$ was adjusted to 0.8 mM by the addition of MgO. The free $[Ca^{2+}]$ was 60 nM. In most experiments, 50 μM *n*-benzyl-*p*-toluene sulfonamide (Calbiochem, Nottingham, UK) was added to inhibit Ca^{2+} activation of the myofilaments (20) and associated movement. All experiments were done at room temperature (20–22 °C), pH 7.1.

A modified Tyrode's "external" solution was used, which comprised (in mM): 140.3 NaCl; 2.48 KCl; 1.5 $CaCl_2$; 1 $MgCl_2$; 5 HEPES; 5 glucose; and 5 sodium pyruvate. A halothane stock solution was prepared in a dimethyl sulfoxide (DMSO). The final concentration of DMSO did not exceed 0.1%. Once prepared, solutions with halothane were contained within airtight syringes with zero dead space to prevent vaporization (21). Stock fluo-5N and fluo-3 (Biotium, Hayward, CA) solutions (1 M) were prepared in deionized water. In some experiments, a STIM1 antibody (20 μg/ml; BD Biosciences, Dorset, UK) was introduced into the t-system before skinning. This antibody targets the extracellular N terminus of STIM1 within the plasma membrane (22).

Western Blot—MHN muscle samples were fractionated using detergent-free methods (23). In brief, peripheral membrane proteins were extracted in 500 mM Na_2CO_3 containing 0.5 mM EGTA and 1% protease inhibitor mixture (Sigma), homogenized, sonicated (three times each for 20 s at full power), and layered on a discontinuous sucrose gradient (45–35-5%). 12 fractions were collected following centrifugation for 17 h (280,000 × *g*) at 4 °C. STIM1 (610954; BD Biosciences), caveolin-3 (610420; BD Biosciences), and β-adaptin (610382; BD Biosciences) were measured by Western blotting following SDS-PAGE. As described recently (24), the STIM1 antibody identified additional bands at two additional bands at ~50 and ~42 kDa in human muscle (not shown). Consequently, although extracellular application of the STIM1 antibody produced a striated pattern consistent with binding to the t-system (supplemental Fig. 1), this finding should be interpreted with caution.

Apparatus—Mechanically skinned muscle fibers were mounted in a shallow bath with a glass coverslip base as described previously (25). The experimental bath was placed on the stage of an S200 Nikon Diaphot inverted microscope (Nikon, Surrey, UK). Muscle fibers were viewed via ×40 Fluor objective (Nikon CF Fluor, NA 0.75). A confocal laser-scanning unit (Cellmap, Bio-Rad, Herts, UK) was attached to the side port of the microscope. Fluorophores were excited with the 488-nm line of a diode laser and emitted fluorescence was measured at >515 nm. In most experiments, the system was configured with a "signal-enhancing lens system" in the light path, which improves detection efficiency while slightly reducing confocality (50). This configuration minimizes bleaching and allows more prolonged scanning of live cells.

Mechanical Skinning and Compartmentalization of fluo-5N within the Resealed T-system—When fibers are mechanically skinned under oil, the necks of the t-tubules close off at the periphery, thereby trapping the extracellular fluid within the resealed t-system (1). Thereafter, the cytosolic space becomes an extension of the bathing solution. There was no apparent difference in susceptibility to damage between MHS and MHN fibers.

Changes in $[Ca^{2+}]$ within the t-system were detected using fluo-5N, which was trapped within the t-system using one of two methods. In the first method, a thin film of external solution containing fluo-5N was introduced at the interface between the fiber and the surrounding oil (1), allowing the dye to enter the t-system before mechanical skinning and resealing. Supplemental Fig. 2*A* shows a confocal *x-y* image (average of four frames) obtained from a human MHN fiber, which was skinned using this method. As indicated by the line profile, the characteristic "M" pattern associated with the t-tubule arrangement in mammalian muscle is clearly visible (26). In other figures shown in this study, the t-tubule pattern is typically less distinct. This is because the frames were not averaged and because of slight movement of the fiber despite the presence of *n*-benzyl-*p*-toluene sulfonamide and the use of the signal-enhancing lens system.

In some experiments, an alternative method was used, which exploits the tendency for fluorophores to be transported from the cytosol to the extracellular space (27). Briefly, skinned fibers

were placed in an internal solution containing 100 μM fluo-5N, which was progressively transported from the cytosol into the t-system. Adequate dye loading was obtained after ~20 min, and uptake into the t-system was potently inhibited by the non-specific anion transport inhibitor probenecid (see supplemental Fig. 3), suggesting the involvement of an anion transporter (27). In all experiments, fluo-5N was removed from the bathing solution for at least 5 min before commencing the experiment, leaving the dye in the t-system only. There was no apparent difference between the properties of SOCE measured using the two methods.

In control experiments with the signal-enhancing lens system lens in place, a slow decrease in t-system fluorescence occurred with time (supplemental Fig. 2*B*). This presumably reflects the combined effects of dye bleaching and loss. All cumulative data graphs were corrected for this loss of t-system fluorescence.

Rationale for SR Ca^{2+} Release Protocols—In previous studies, we have characterized the effects of both halothane and sevoflurane on RyR1 activation in human MHS and MHN skinned fibers (21, 28). Once triggered, the properties of SR Ca^{2+} release are similar with both anesthetics, although the probability of triggering release is lower with sevoflurane (28). In the clinical setting, sevoflurane is the more commonly used volatile anesthetic. However, halothane was used in the present study (i) because it induces SR Ca^{2+} release more consistently than sevoflurane in MHS muscle and (ii) because single fiber data can be compared with the IVCT from the same patient, where the dose-response relationship to halothane is the basis of the standardized diagnostic test.

Halothane was applied at 0.5 mM, which is within the range that occurs clinically during anesthetic induction (29) (and therefore known to induce MH) but does not normally trigger SR Ca^{2+} release in MHN fibers. In experiments involving cytosolic Ca^{2+} measurement (see Fig. 1), a maximal SR Ca^{2+} depletion was induced by rapid exposure to 20 mM caffeine, whereas simultaneously decreasing the free [Mg^{2+}] to 20 μM. However, in experiments involving SOCE where *x-y* images were taken (see Figs. 2–4), maximal SR Ca^{2+} depletion was induced by decreasing the free [Mg^{2+}] to 20 μM alone (30). Although less rapid, this method of SR Ca^{2+} depletion was preferred because it minimized movement associated with myofilament activation.

Data Analysis—Analysis was done using Image Pro Plus (Media Cybernetics) and Image J software (National Institutes of Health). The change in t-tubule fluorescence was expressed as a percentage of the maximum steady-state fluorescence immediately prior to induction of SOCE. The zero point was taken to be that remaining after the fiber had been exposed to 50 μg/ml saponin for 10 min to permeabilize the t-system. In the cumulative data, each point represents the average pixel value of the corresponding *x-y* frame. Data are presented as the mean ± S.E., with the number of observations indicated in parentheses (*n*). Statistical significance ($p < 0.05$) was determined using a one-way analysis of variance. All statistical analysis was performed using Origin software (MicroCal).

RESULTS

Halothane Sensitivity of MHS and MHN Fibers—Initial experiments were done to establish whether the differential halothane sensitivity of MHN and MHS muscle apparent in the diagnostic IVCT could be demonstrated in skinned fibers (Fig. 1*A*). After skinning, both MHN and MHS fibers were perfused for 5 min with a weakly Ca^{2+}-buffered intracellular solution. A solution containing 20 mM caffeine and 20 μM [Mg^{2+}] (low Mg^{2+}) was then applied until the response reached a maximal level after ~10 s. The amplitude of the resulting fluo-3 fluorescence transient was used as an index of the SR Ca^{2+} content. A further ~5-min perfusion was typically sufficient to allow the SR to re-reload to a similar level, as indicated by the amplitude of the second response to 20 mM caffeine/low Mg^{2+}. Using this SR Ca^{2+} load and release protocol, several reproducible Ca^{2+} transients could be obtained with little change in the amplitude or time course of the response.

After reloading the SR for a third time, fibers were subjected to stepwise increases in [halothane] over the range 0.2–5 mM or until SR Ca^{2+} release occurred. In MHN fibers (*upper panel*), SR Ca^{2+} release consistently occurred at ≥2 mM halothane under these conditions. In contrast, MHS fibers typically exhibited a robust SR Ca^{2+} release at ≤0.5 mM halothane (*lower panel*). Following exposure to halothane, the SR was reloaded, and a final maximal SR Ca^{2+} release was induced to confirm the viability of the preparation.

In ~10% of MHS fibers, the SR Ca^{2+} release induced by halothane took the form of a propagated cytosolic Ca^{2+} wave. Fig. 1*B* shows sequential *x-y* confocal images obtained from an MHS fiber under control conditions and following the introduction of 0.5 mM halothane. Application of halothane was associated with SR Ca^{2+} release, which originated outside the field of view and propagated from right to left in sequential images, consistent with Ca^{2+}-induced Ca^{2+} release. As in previous studies (21), propagated SR Ca^{2+} release was not observed in MHN fibers under these conditions.

Cumulative data showing the number of MHS and MHN fibers that exhibited SR Ca^{2+} release in response to 0.5 mM halothane under control conditions and in the presence of 0.8 mM Mg^{2+} or 0.2 mM Mg^{2+} is shown in Fig. 1*C*. At 0.8 mM $[Mg^{2+}]_i$, a level within the normal physiological range (31), 0.5 mM halothane discriminated effectively between MHS and MHN fibers with 8/8 and 1/8 fibers responding to 0.5 mM halothane, respectively. Consistent with previous studies on human fibers (32), a decrease in the cytosolic [Mg^{2+}] to 0.2 mM increased the responsiveness of MHN fibers to the anesthetic such that 0.5 mM halothane induced SR Ca^{2+} release in all MHS and MHN fibers.

Although one MHN fiber responded unexpectedly to 0.5 mM halothane, these data on skinned fibers demonstrate a high degree of consistency with the IVCT diagnosis. Therefore, as 0.5 mM halothane is also within the range expected to occur during anesthetic induction (29), this concentration was used in all subsequent experiments.

Evidence of SOCE in Human MHS and MHN Fibers—Experiments were carried out to establish whether the SR Ca^{2+} release induced by volatile anesthetic exposure (Fig. 1) triggers

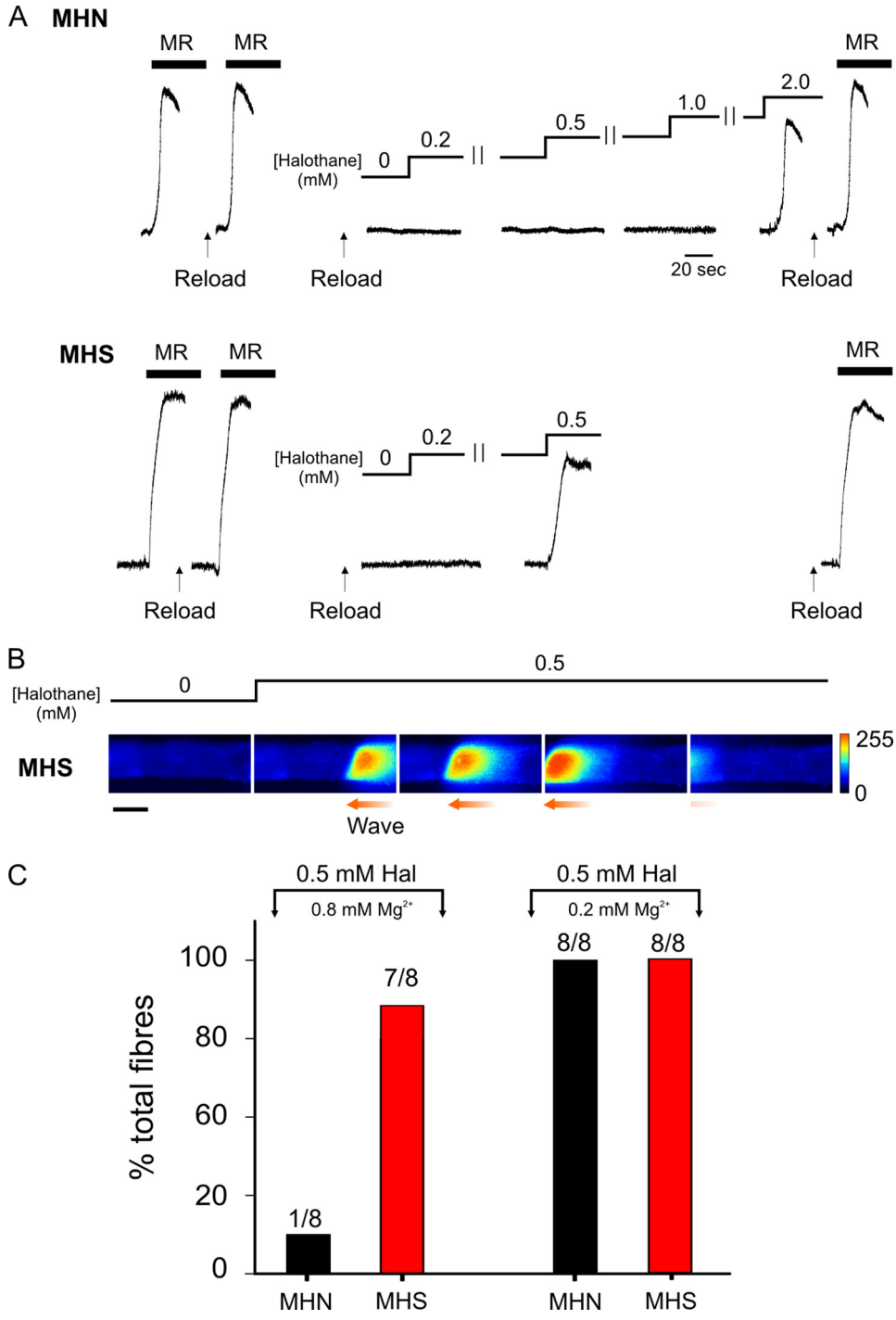

FIGURE 1. **Differential sensitivity of cytosolic SR Ca^{2+} release to halothane in MHS and MHN fibers.** *A*, typical example showing an endogenously Ca^{2+}-loaded MHN fiber, which was initially exposed to a solution containing 20 mM caffeine and 20 μM Mg^{2+} to induce a maximal release (*MR*) of Ca^{2+} from the SR, resulting in a transient increase in fluo-3 fluorescence within the cytosol (*upper panel*). The SR was then reloaded to the same by exposure to a solution with a free [Ca^{2+}] of ~200 nM, and another maximal Ca^{2+} release was induced. After reloading the SR again, the MHN fiber was subjected to stepwise increases in [halothane] until SR Ca^{2+} release occurred at 2 mM in this example. When the same protocol was applied to MHS fibers, the threshold for halothane-induced Ca^{2+} release was consistently ≤0.5 mM (*lower panel*). *B*, sequential *x-y* confocal images (0.83 Hz) from an MHS fiber in which halothane exposure induced a slow propagated Ca^{2+} wave. *Scale bar* indicates 80 μm. *C*, cumulative data showing the proportion of MHS and MHN fibers responding to 0.5 mM halothane in the presence of 0.8 or 0.2 mM Mg^{2+}. The total number of halothane-responsive fibers (one per patient) is indicated above each bar.

Ca^{2+} influx via SOCE. MHN or MHS fibers were mechanically skinned, and fluo-5N was trapped within the resealed t-system (see "Experimental Procedures"). In this and all subsequent protocols addressing SOCE, dyes were absent from the cytosol. Fig. 2*A* shows representative confocal *x-y* images of fluo-5N trapped with the resealed t-system of an MHN (*upper panel*) and an MHS (*lower panel*) human skeletal muscle fiber. In the MHN fiber, rapidly increasing [halothane] to 0.5 mM for 60 s had no apparent effect on fluo-5N fluorescence. However, a subsequent maximal SR Ca^{2+} release induced by a decrease in the [Mg^{2+}] from 0.8 mM to 20 μM (30) was associated with a pronounced reduction in fluo-5N fluorescence, consistent with SOCE. In contrast, exposure of the MHS fiber to 0.5 mM halothane caused a transient increase in [Ca^{2+}] within the resealed t-system ($[Ca^{2+}]_{t\text{-}sys}$) followed by a gradual decrease due to SOCE. A subsequent maximal SR Ca^{2+} release induced a further depletion of $Ca^{2+}{}_{t\text{-}sys}$, indicating that the effect of 0.5 mM halothane on SOCE was submaximal.

Cumulative data showing the time-dependent effects of halothane on fluo-5N fluorescence are given in Fig. 2*B*. MHN fibers consistently failed to respond to 0.5 mM halothane. However, in MHS fibers, fluorescence transiently increased on halothane exposure to 107 ± 1.2% (n = 8) before decreasing toward a new steady-state level (69 ± 3.6%, n = 8) after ~60 s. In both MHN and MHS fibers, maximal depletion of SR Ca^{2+} ([Mg^{2+}] reduced to 20 μM) decreased the fluo-5N fluorescence to 20 ± 1.5 and 21 ± 2% of the control value, respectively. These values were not significantly different ($p > 0.05$).

Halothane Induced Waves of SOCE in Human MHS Fibers—As shown in Fig. 1*B*, in some MHS fibers, SR Ca^{2+} release took the form of a propagated cytosolic Ca^{2+} wave. Fig. 3 shows a series of *x-y* images rendered as surface plots, obtained from an MHS fiber following the introduction of 0.5 mM halothane. This example clearly shows a wave crest of raised $[Ca^{2+}]_{t\text{-}sys}$, which propagated from right to left. As in Fig. 2, the initial increase in $Ca^{2+}{}_{t\text{-}sys}$ was followed by a sustained decrease, consistent with SOCE. Although cyto-

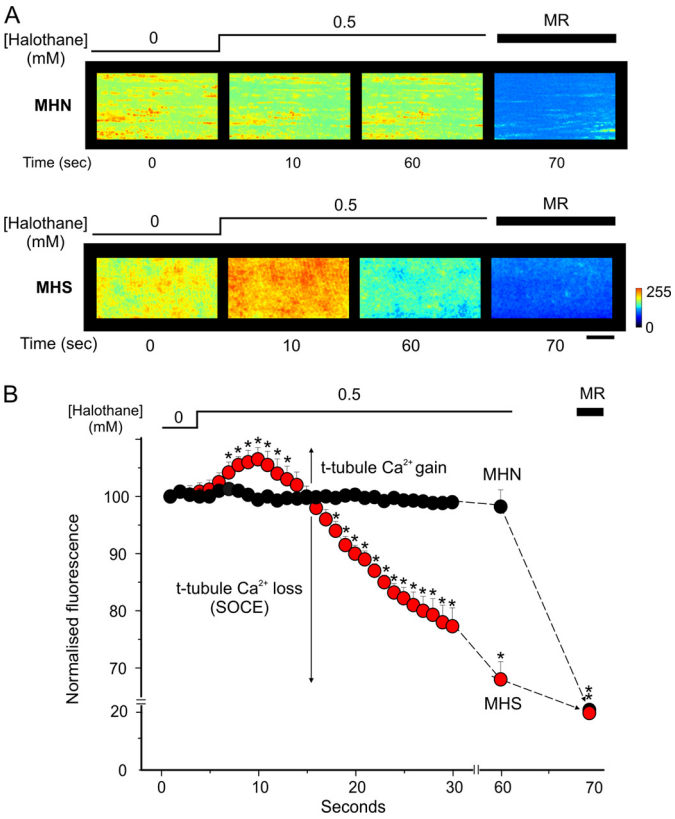

FIGURE 2. **Properties of halothane-induced SOCE.** *A*, typical *x-y* confocal images of fluo-5N fluorescence obtained with the dye trapped within the resealed t-tubules of a mechanically skinned MHN or MHS fiber. In MHN fibers (*upper panel*), the introduction of 0.5 mM halothane had no apparent effect on fluo-5N fluorescence within 60 s. However, after initiation of a maximal SR Ca^{2+} release (*MR*) by reducing in the free $[Mg^{2+}]$ to 20 μM, t-tubule fluorescence decreased markedly. In MHS fibers (*lower panel*), the introduction of 0.5 mM halothane resulted in an initial increase in fluo-5N fluorescence followed by a decrease, which approached a new steady state after ~60 s. Thereafter, initiation of a maximal SR Ca^{2+} release induced a further decrease in fluo-5N fluorescence. *B*, cumulative data showing the mean fluorescence obtained from sequential *x-y* images before and during exposure to halothane or maximal SR Ca^{2+} release (*MR*), in MHS ($n = 8$, *red circles*) or MHN ($n = 8$, *black circles*) human skeletal muscle fibers. Each data point represents mean ± S.E. * indicates significantly different from control, $p < 0.05$.

solic Ca^{2+} could not be imaged simultaneously in this study, it seems likely that the wave of $[Ca^{2+}]_{t\text{-}sys}$ change was secondary to a wave of SR Ca^{2+} release (Fig. 1*B*). Similar results were obtained in two other preparations.

Effects of Mg^{2+} on Halothane-induced SOCE in MHN Fibers—Previous work has shown that in fibers from MHN patients, decreasing the $[Mg^{2+}]_i$ facilitates Ca^{2+}-induced Ca^{2+} release and increases the sensitivity of RyR1 to halothane (28). As shown in Fig. 1*C*, decreasing $[Mg^{2+}]$ from 0.8 to 0.2 mM normalized the responses such that all MHN and MHS fibers exhibited SR Ca^{2+} release on the introduction of 0.5 mM halothane (Fig. 1*C*). Fig. 4*A* shows representative *x-y* images from an MHN fiber perfused continuously with a solution containing 0.2 mM $[Mg^{2+}]$. The introduction of 0.5 mM halothane induced a transient increase in t-tubule fluorescence followed by a sustained decrease, consistent with SOCE. This response to halothane in MHN fibers at 0.2 mM Mg^{2+} was qualitatively similar to that obtained in MHS fibers at 0.8 mM Mg^{2+} (Fig. 2*A*). The cumulative data show that in the presence of 0.2 mM Mg^{2+}, MHN fibers exhibit a transient increase in fluorescence to 107 ± 2.7% ($n = 8$) after ~5 s of exposure to halothane, before decreasing to 73 ± 9% after 60 s (Fig. 4*B*). Again, there was no significant effect of 0.5 mM halothane in the presence of 0.8 mM Mg^{2+}.

Effects of STIM1 Antibody on SOCE in MHS Fibers—STIM1 is located within SR/endoplasmic reticulum membrane, where it acts as a Ca^{2+} sensor, communicating store depletion to sarcolemmal store-operated Ca^{2+} channels (31, 33). However, recent work suggests that STIM1 is also present within the sarcolemma in some cell types and that inhibition of the protein with a blocking antibody can inhibit SOCE (22, 34). As STIM1 is present in skeletal muscle sarcolemma (36), experiments were carried out to establish whether extracellular application of a STIM1-blocking antibody influences SOCE in human muscle.

When the STIM1-blocking antibody was trapped within the resealed t-system before exposure of an MHS fiber to 0.5 mM halothane, the initial increase in t-system fluorescence was unaffected (Fig. 5*A*, *upper panel*). Thereafter, however, although the fluorescence gradually decayed toward the control level, there was no significant depletion of $Ca^{2+}{}_{t\text{-}sys}$ within 60 s. In contrast, when the antibody was denatured prior to application (see "Experimental Procedures"), 0.5 mM halothane induced a typical SOCE response, *i.e.* t-system fluorescence initially increased and peaked after ~5 s before decreasing toward a new steady-state after 60 s (*lower panel*).

In Fig. 5*B*, the cumulative data showing the characteristic response to 0.5 mM halothane in MHS fibers are shown superimposed upon the data obtained with the STIM1 antibody present within the sealed t-system. The persistence of the initial rising phase following antibody exposure suggests that SR Ca^{2+} release and subsequent efflux into the t-system are unaffected by the STIM1 antibody, whereas Ca^{2+} efflux due to store depletion is markedly inhibited. Indeed, the fluorescence after 60 s was not significantly different from the control value prior to halothane exposure ($p > 0.05$, $n = 8$). However, SOCE was not inhibited when the antibody was denatured by heating. In further control experiments involving measurement of cytosolic $[Ca^{2+}]$, the STIM1 antibody did not affect SR Ca^{2+} release induced by either caffeine or halothane (not shown).

A typical Western blot obtained from human vastus medialis (Fig. 5*C*) confirms the presence of STIM1 in whole muscle homogenate. STIM1 is also enriched in fraction 6, which is a buoyant fraction containing cholesterol-enriched sarcolemma (lipid rafts and caveolae). Note the relative absence of β-adaptin (a marker of non-raft membranes) in fractions 5 and 6, whereas caveolin-3 (a marker of caveolae) is enriched.

DISCUSSION

This is the first study to demonstrate 1) SOCE in adult human skeletal muscle and 2) sustained sarcolemmal Ca^{2+} influx in MHS muscle, under conditions that precipitate pathological SR Ca^{2+} release. In both MHN and MHS fibers, changes in t-system $[Ca^{2+}]$ only occurred under conditions that precipitated SR Ca^{2+} depletion, *e.g.* in MHS muscle fibers, where 0.5 mM halothane consistently induced SR Ca^{2+} release (Fig. 1), the introduction of the anesthetic caused an initial rise in $[Ca^{2+}]_{t\text{-}sys}$ followed by a sustained decrease (Fig. 2, *A* and *B*). In MHN fibers, halothane consistently failed to initiate SR Ca^{2+}

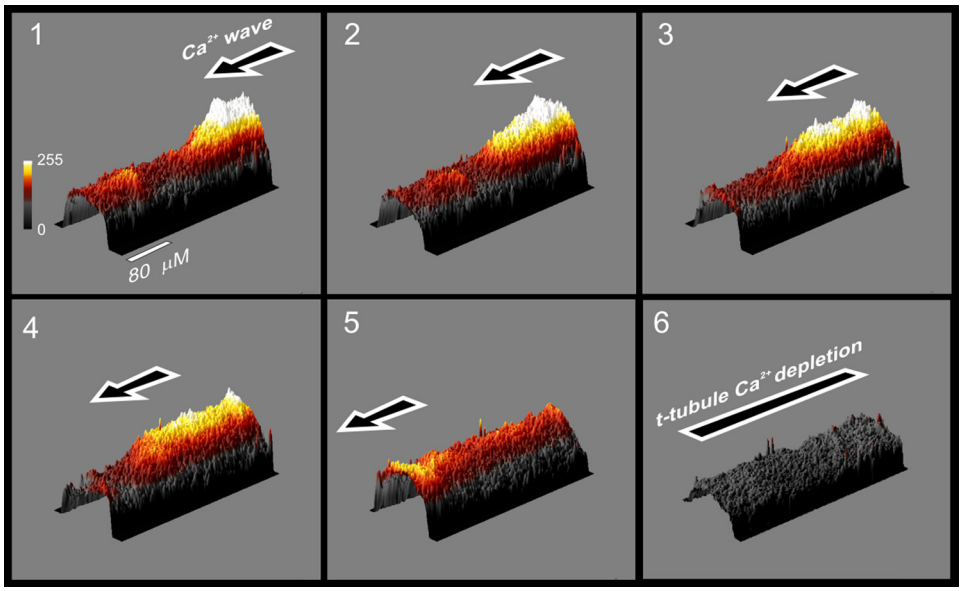

FIGURE 3. **Halothane-induced wave of SOCE in human MHS fibers.** Sequential surface plots of *x-y* confocal images taken from an MHS fiber (0.83 Hz), which exhibited a propagated wave of t-tubule $[Ca^{2+}]$ change following exposure to 0.5 mM halothane, are shown. An initial wave front of raised $[Ca^{2+}]_{t\text{-}sys}$ was followed by sustained $[Ca^{2+}]_{t\text{-}sys}$ depletion. Similar results were obtained in two other preparations.

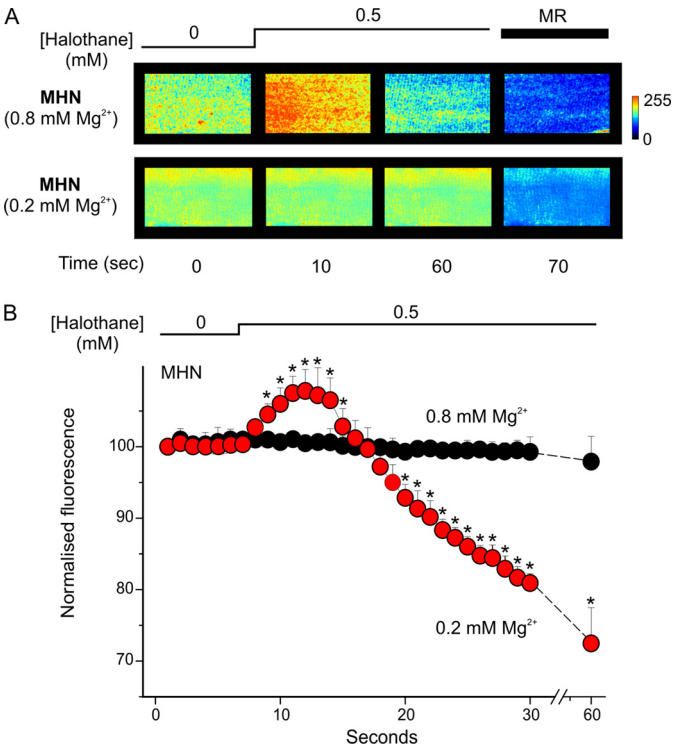

FIGURE 4. **Effect of reduced $[Mg^{2+}]$ on the response of MHN fibers to halothane.** *A*, typical *x-y* confocal images of fluo-5N fluorescence within the resealed t-tubules of a skinned MHN fiber in the presence of 0.8 mM (*upper panel*) or 0.2 mM Mg^{2+} (*lower panel*) free $[Mg^{2+}]$. At 0.8 mM Mg^{2+}, halothane had no apparent effect on fluo-5N fluorescence, whereas a subsequent maximal SR Ca^{2+} release (*MR*) induced a sustained decrease in $[Ca^{2+}]_{t\text{-}sys}$. In the presence of 0.2 mM Mg^{2+}, the introduction of halothane resulted in a transient increase in $[Ca^{2+}]_{t\text{-}sys}$ followed by a sustained decrease. *B*, cumulative data showing the mean fluorescence obtained from sequential *x-y* images before and during exposure to 0.5 mM halothane in the presence of 0.8 mM ($n = 8$, *red circles*) or 0.2 mM ($n = 8$, *black circles*) free Mg^{2+}. Each data point represents mean ± S.E. * indicates significantly different from control, $p < 0.05$.

release (Fig. 1*A*), or to induce changes in t-system $[Ca^{2+}]$ (Fig. 2, *A* and *B*).

When MHN fibers were perfused with a reduced level of cytosolic $[Mg^{2+}]$ (0.2 mM), halothane induced both SR Ca^{2+} release (Fig. *1C*) and changes in $[Ca^{2+}]_{t\text{-}sys}$, similar to those obtained in MHS fibers (Fig. 4). This effect of low $[Mg^{2+}]$ on MHN fibers likely reflects the fact that RyR1 gating is potently inhibited by Mg^{2+} in resting skeletal muscle (30). Decreasing the $[Mg^{2+}]$ to 0.2 mM is sufficient to facilitate agonist-induced activation of RyR1 but does not itself cause loss of Ca^{2+} from the SR (21). The fact that SOCE can be induced in MHN fibers by facilitating halothane-induced SR Ca^{2+} release suggests that the phenomenon occurs due to store depletion and is not a unique characteristic of MH or particular RYR1 mutations. This conclusion is supported by the fact that the RYR1 mutations identified in the present study are spread throughout all three hot spot regions of RYR1 (see supplemental Table 1).

The characteristic biphasic change in $[Ca^{2+}]_{t\text{-}sys}$ that occurred in MHS fibers in response to halothane is qualitatively similar to that reported in mechanically skinned rat skeletal muscle fibers following the addition of caffeine and/or inhibition of sarcoplasmic reticulum Ca^{2+}-ATPase (3). The initial increase in $[Ca^{2+}]_{t\text{-}sys}$ can be explained if sarcolemmal Ca^{2+} extrusion mechanisms facilitate a net efflux of Ca^{2+} from the cytosol into the t-system when cytosolic $[Ca^{2+}]$ is raised. Consistent with this, previous studies have shown that the initial transient rise in $[Ca^{2+}]_{t\text{-}sys}$ can be abolished by raising the Ca^{2+} buffer capacity of the cytosolic medium (3). The later sustained decrease in $[Ca^{2+}]_{t\text{-}sys}$ can be explained by a Ca^{2+} flux from the sealed t-system into the cytosolic space, triggered by depletion of SR Ca^{2+}, *i.e.* SOCE. However, subsequent maximal depletion of SR Ca^{2+} induced a further decrease in $[Ca^{2+}]_{t\text{-}sys}$, suggesting that SOCE was not fully activated by halothane (Fig. 2, *A* and *B*).

Waves of T-tubule Ca^{2+} Depletion—Previous studies have reported markedly different rates of SOCE in skinned skeletal muscle fibers, *e.g.* Brotto and colleagues (7, 10, 37, 38) reported that $[Ca^{2+}]_{t\text{-}sys}$ declined slowly in murine skeletal muscle, only approaching a new steady-state 8–10 min after initiation of SR Ca^{2+} release. In contrast, Launikonis and Ríos (3) reported a much more rapid depletion of $[Ca^{2+}]_{t\text{-}sys}$ in rat fibers, which was detectable within 1 s of SR Ca^{2+} release and declined toward a new steady state over ~30–50 s. These apparent differences in the temporal properties of SOCE might reflect species variation or aspects of the methodology, *e.g.* the rate of solution exchange or inadequate compensation for dye loss/bleaching. However, the present study on human skeletal muscle clearly demonstrates a rapid Ca^{2+}

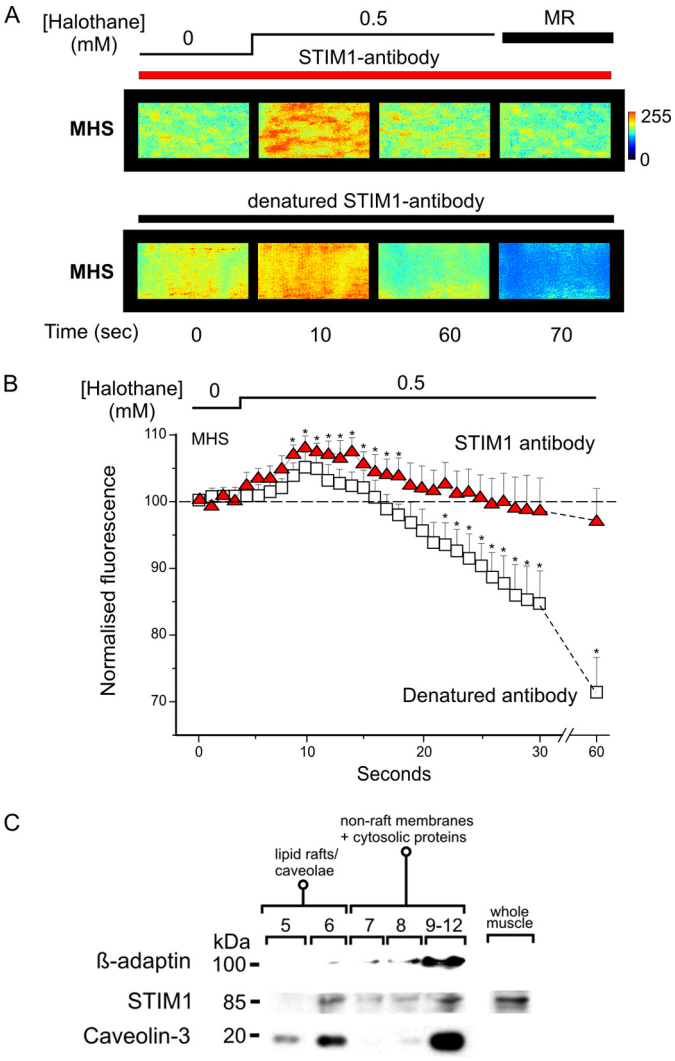

FIGURE 5. **Effects of STIM1 antibody on the response of MHS fibers to halothane.** *A*, *x-y* confocal images of fluo-5N fluorescence within the resealed t-tubules of a skinned MHS fiber in which a STIM1 antibody had been introduced into the t-system prior to skinning. In this case, exposure to halothane was followed by a characteristic increase in $[Ca^{2+}]_{t\text{-}sys}$ (*upper panel*). However, fluo-5N fluorescence then returned slowly toward the control level, and there was little evidence of a sustained decrease within 60 s or subsequently after a maximal SR Ca^{2+} release (*MR*). This procedure was repeated in an MHS fiber using a sample of the antibody, which had been denatured by heating (*lower panel*). After heat treatment, application of halothane resulted in a typical SOCE response. *B*, cumulative data showing the mean fluorescence obtained from sequential *x-y* images in MHS fibers with either the active STIM1 antibody ($n = 8$, *red triangles*) or the denatured antibody ($n = 8$, *open squares*) trapped within the t-system. * indicates statistically different from control level, $p < 0.05$. *C*, representative Western blot from human vastus medialis muscle. STIM1 is indentified in whole muscle human homogenate and is also enriched in the buoyant fraction 6, which contains sarcolemmal lipid rafts and caveolae. β-Adaptin (a marker of non-raft membranes) is present at low levels in fractions 5 and 6, whereas caveolin-3 (a marker of caveolae) is enriched. Fractions 7–12 are mostly non-raft membranes and cytosolic proteins. Unlike some other caveolin isoforms, caveolin-3 is found outside buoyant membrane fractions as observed here in fractions 9–12 (35).

flux associated with SOCE, which occurred on a similar time scale to that described by Launikonis and Ríos in rat muscle (Fig. 2*B*) (3). Furthermore, we show for the first time that in MHS fibers, waves of $[Ca^{2+}]_{t\text{-}sys}$ depletion (Fig. 3) can occur on a similar tine course to halothane-induced SR Ca^{2+} waves (Fig. 1*B*), suggesting a causal relationship. This further emphasizes the close temporal coupling between SR Ca^{2+} release and activation of SOCE.

STIM1 and SOCE in Skeletal Muscle—Recent findings implicate STIM1 and Orai1 as key molecular components underlying SOCE in skeletal muscle, *e.g.* (i) SOCE is abolished following STIM1 knockdown or by expression of a dominant negative/permeation-defective Orai1 (39) and (ii) myotubes from mice lacking functional STIM1 exhibit defects in force generation and impaired fatigue resistance (36). These and related findings have led to the suggestion that in skeletal muscle, STIM functions as the SR Ca^{2+} sensor, whereas Orai1 mediates sarcolemmal Ca^{2+} influx during SOCE, either alone acting as the Ca^{2+} release-activated Ca^{2+} channel or in combination with other channels (36). Interestingly, STIM1 has been identified within the plasma membrane in a number of cell types including human epidermal cancer cells, HEK293 cells, and vascular smooth muscle cells (22, 34, 40, 41) These studies also showed that extracellular application of the BD Biosciences STIM1 antibody can inhibit SOCE.

A previous study on rabbit skeletal muscle identified STIM1 in t-tubule membranes (36), and the present findings on human muscle confirm its presence in a buoyant sarcolemmal fraction enriched with lipid rafts and caveolae (Fig. 5*C*). Furthermore, trapping the STIM1 antibody within the sealed t-system markedly inhibited the SOCE response to halothane in human MHS fibers (Fig. 5*A*). The initial transient increase in $[Ca^{2+}]_{t\text{-}sys}$ was, however, unaffected by the antibody, suggesting that SR Ca^{2+} release had occurred. SR Ca^{2+} release was not affected by the antibody, and denaturing the protein abolished its inhibitory effect (Fig. 5*B*). On balance, previous work suggests that sarcolemmal STIM1 modulates but is not essential for SOCE (42). Nevertheless, inhibition of SOCE by application of an extracellular antibody provides a novel approach to studying the role of SOCE in adult skeletal muscle, where other commonly used inhibitors (*e.g.* 2-APB) are ineffective.[3]

Relationship to Previous Studies—In addition to SOCE, two other forms of Ca^{2+} influx have been identified in skeletal muscle. "Excitation-coupled Ca^{2+} entry" (ECCE) has mostly been characterized in myotubes and is triggered by repeated or sustained membrane depolarization (43). ECCE does not require store depletion and probably occurs via the L-type Ca^{2+} channel (43–45). More recently, a "t-system action potential-activated Ca^{2+} current" (APACC) has been described in adult rat skeletal muscle (6). APACC differs from ECCE in that it is activated by a single action potential but inactivated by repeated depolarizations. These forms of Ca^{2+} entry are distinct from SOCE, which does not require membrane depolarization, is initiated by SR Ca^{2+} depletion to a threshold level, and is only inactivated by store refilling (2, 3, 6).

As the Ca^{2+} fluxes associated with both APACC and ECCE require depolarization, these mechanisms may play a physiological role during normal patterns of activity by correcting any efflux of Ca^{2+} from the cell that occurs via sarcolemmal Ca^{2+} extrusion mechanisms (6, 44). Interestingly, it has been reported that ECCE is enhanced in myotubes from mice with

[3] A. M. Duke, P. M. Hopkins, S. C. Calaghan, J. P. Halsall, and D. S. Steele, unpublished observations.

the R163C RyR1 MH mutation (46). As sarcolemmal depolarization and consequent fasciculations are known to occur in the presence of the muscle relaxant succinylcholine (47), enhanced ECCE current might contribute to the rise in cytosolic [Ca^{2+}] that underlies MH.

SOCE does not appear to be activated during individual twitch or tetanic responses (3, 48) but might play a role in fatigue (49), where substantial SR Ca^{2+} depletion can occur (8). Importantly, the present data also suggest that in human MHS muscle, a level of halothane (0.5 mM) within the concentration range that occurs during anesthetic induction (29) can induce sufficient SR Ca^{2+} depletion to activate SOCE. Such an effect could be large enough to adversely affect cell function. In normal mammalian skeletal muscle, the Ca^{2+} flux associated with SOCE has been calculated to be $\sim$19 μM s^{-1}, which corresponds to 1.1–2.2 mM Ca^{2+} within 1–2 min (3), sufficient to completely refill the SR within this period (2). Furthermore, given the properties of SOCE, Ca^{2+} influx would be expected to continue until the SR Ca^{2+} content is restored despite persistent RyR1 activation. On this basis, we propose that sarcolemmal Ca^{2+} influx via SOCE likely contributes to the sustained increase in cytosolic [Ca^{2+}] that underlies MH.

Summary—We show for the first time in human MHS skeletal muscle that (i) a level of halothane within the range that occurs during anesthesia induces sufficient SR Ca^{2+} release to activate SOCE; (ii) waves of SR Ca^{2+} release can induce corresponding waves of $Ca^{2+}_{t\text{-}sys}$ depletion, suggesting a close temporal relationship between Ca^{2+} release and SOCE; and (iii) extracellular application of a STIM1-blocking antibody potently inhibits the decrease in $[Ca^{2+}]_{t\text{-}sys}$, suggesting that sarcolemmal STIM1 has an important modulatory role in SOCE. Finally, we suggest that during an MH episode, SOCE may contribute to and sustain the pathological increase in cytosolic [Ca^{2+}].

Acknowledgment—We thank Professor David Beech for advice during this study.

REFERENCES

1. Launikonis, B. S., Barnes, M., and Stephenson, D. G. (2003) *Proc. Natl. Acad. Sci. U.S.A.* **100,** 2941–2944
2. Kurebayashi, N., and Ogawa, Y. (2001) *J. Physiol.* **533,** 185–199
3. Launikonis, B. S., and Ríos, E. (2007) *J. Physiol.* **583,** 81–97
4. Posterino, G. S., and Lamb, G. D. (2003) *J. Physiol.* **551,** 219–237
5. Launikonis, B. S., Zhou, J., Royer, L., Shannon, T. R., Brum, G., and Ríos, E. (2006) *Proc. Natl. Acad. Sci. U.S.A.* **103,** 2982–2987
6. Launikonis, B. S., Stephenson, D. G., and Friedrich, O. (2009) *J. Physiol.* **587,** 2299–2312
7. Zhao, X., Yoshida, M., Brotto, L., Takeshima, H., Weisleder, N., Hirata, Y., Nosek, T. M., Ma, J., and Brotto, M. (2005) *Physiol. Genomics* **23,** 72–78
8. Kabbara, A. A., and Allen, D. G. (2001) *J. Physiol.* **534,** 87–97
9. Steele, D. S., and Duke, A. M. (2003) *Acta Physiol. Scand.* **179,** 39–48
10. Zhao, X., Weisleder, N., Thornton, A., Oppong, Y., Campbell, R., Ma, J., and Brotto, M. (2008) *Aging Cell* **7,** 561–568
11. MacLennan, D. H., Duff, C., Zorzato, F., Fujii, J., Phillips, M., Korneluk, R. G., Frodis, W., Britt, B. A., and Worton, R. G. (1990) *Nature* **343,** 559–561
12. McCarthy, T. V., Healy, J. M., Heffron, J. J., Lehane, M., Deufel, T., Lehmann-Horn, F., Farrall, M., and Johnson, K. (1990) *Nature* **343,** 562–564
13. Adnet, P. J., Krivosic-Horber, R. M., Adamantidis, M. M., Reyford, H., Cordonnier, C., and Haudecoeur, G. (1991) *Anesthesiology* **75,** 413–419
14. Fletcher, J. E., Huggins, F. J., and Rosenberg, H. (1990) *Can. J. Anaesth.* **37,** 695–698
15. Brum, G., Ríos, E., and Stéfani, E. (1988) *J. Physiol.* **398,** 441–473
16. The European Malignant Hyperpyrexia Group (1984) *Br. J. Anaesth.* **56,** 1267–1269
17. Ording, H., Brancadoro, V., Cozzolino, S., Ellis, F. R., Glauber, V., Gonano, E. F., Halsall, P. J., Hartung, E., Heffron, J. J., Heytens, L., Kozak-Ribbens, G., Kress, H., Krivosic-Horber, R., Lehmann-Horn, F., Mortier, W., Nivoche, Y., Ranklev-Twetman, E., Sigurdsson, S., Snoeck, M., Stieglitz, P., Tegazzin, V., Urwyler, A., and Wappler, F. (1997) *Acta Anaesthesiol. Scand.* **41,** 955–966
18. Robinson, R., Carpenter, D., Shaw, M. A., Halsall, J., and Hopkins, P. (2006) *Hum. Mutat.* **27,** 977–989
19. Lynch, G. S., Stephenson, D. G., and Williams, D. A. (1995) *J. Muscle Res. Cell Motil.* **16,** 65–78
20. Cheung, A., Dantzig, J. A., Hollingworth, S., Baylor, S. M., Goldman, Y. E., Mitchison, T. J., and Straight, A. F. (2002) *Nat. Cell Biol.* **4,** 83–88
21. Duke, A. M., Hopkins, P. M., Halsal, J. P., and Steele, D. S. (2004) *Anesthesiology* **101,** 1339–1346
22. Spassova, M. A., Soboloff, J., He, L. P., Xu, W., Dziadek, M. A., and Gill, D. L. (2006) *Proc. Natl. Acad. Sci. U.S.A.* **103,** 4040–4045
23. Calaghan, S., Kozera, L., and White, E. (2008) *J. Mol. Cell Cardiol.* **45,** 88–92
24. Edwards, J. N., Murphy, R. M., Cully, T. R., von Wegner, F., Friedrich, O., and Launikonis, B. S. (2010) *Cell Calcium* **47,** 458–467
25. Duke, A. M., and Steele, D. S. (1998) *Pflugers Arch.* **436,** 104–111
26. Launikonis, B. S., and Stephenson, D. G. (2002) *Cell Biol. Int.* **26,** 921–929
27. Di Virgilio, F., Fasolato, C., and Steinberg, T. H. (1988) *Biochem. J.* **256,** 959–963
28. Duke, A. M., Hopkins, P. M., Halsall, P. J., and Steele, D. S. (2006) *Br. J. Anaesth.* **97,** 320–328
29. Davies, D. N., Steward, A., Allott, P. R., and Mapleson, W. W. (1972) *Br. J. Anaesth.* **44,** 548–550
30. Lamb, G. D., and Stephenson, D. G. (1994) *J. Physiol.* **478,** 331–339
31. Westerblad, H., and Allen, D. G. (1992) *J. Physiol.* **453,** 413–434
32. Steele, D. S., and Duke, A. M. (2007) *Arch. Biochem. Biophys.* **458,** 57–64
33. Zhang, S. L., Yu, Y., Roos, J., Kozak, J. A., Deerinck, T. J., Ellisman, M. H., Stauderman, K. A., and Cahalan, M. D. (2005) *Nature* **437,** 902–905
34. Dziadek, M. A., and Johnstone, L. S. (2007) *Cell Calcium* **42,** 123–132
35. Head, B. P., Patel, H. H., Roth, D. M., Lai, N. C., Niesman, I. R., Farquhar, M. G., and Insel, P. A. (2005) *J. Biol. Chem.* **280,** 31036–31044
36. Stiber, J., Hawkins, A., Zhang, Z. S., Wang, S., Burch, J., Graham, V., Ward, C. C., Seth, M., Finch, E., Malouf, N., Williams, R. S., Eu, J. P., and Rosenberg, P. (2008) *Nat. Cell Biol.* **10,** 688–697
37. Hirata, Y., Brotto, M., Weisleder, N., Chu, Y., Lin, P., Zhao, X., Thornton, A., Komazaki, S., Takeshima, H., Ma, J., and Pan, Z. (2006) *Biophys. J.* **90,** 4418–4427
38. Zhao, X., Weisleder, N., Han, X., Pan, Z., Parness, J., Brotto, M., and Ma, J. (2006) *J. Biol. Chem.* **281,** 33477–33486
39. Lyfenko, A. D., and Dirksen, R. T. (2008) *J. Physiol.* **586,** 4815–4824
40. Zimina, O. A., Glushankova, A., Skopin, A. Y., Alexeenko, V. A., Vigont, V. A., Mozhayeva, G. N., and Kaznacheyeva, E. V. (2008) *Dokl. Biol. Sci.* **420,** 214–217
41. Li, J., Sukumar, P., Milligan, C. J., Kumar, B., Ma, Z. Y., Munsch, C. M., Jiang, L. H., Porter, K. E., and Beech, D. J. (2008) *Circ. Res.* **103,** e97–104
42. Hewavitharana, T., Deng, X., Wang, Y., Ritchie, M. F., Girish, G. V., Soboloff, J., and Gill, D. L. (2008) *J. Biol. Chem.* **283,** 26252–26262
43. Cherednichenko, G., Hurne, A. M., Fessenden, J. D., Lee, E. H., Allen, P. D., Beam, K. G., and Pessah, I. N. (2004) *Proc. Natl. Acad. Sci. U.S.A.* **101,** 15793–15798
44. Hurne, A. M., O'Brien, J. J., Wingrove, D., Cherednichenko, G., Allen, P. D., Beam, K. G., and Pessah, I. N. (2005) *J. Biol. Chem.* **280,**

36994–37004
45. Bannister, R. A., Pessah, I. N., and Beam, K. G. (2009) *J. Gen. Physiol.* **133,** 79–91
46. Cherednichenko, G., Ward, C. W., Feng, W., Cabrales, E., Michaelson, L., Samso, M., López, J. R., Allen, P. D., and Pessah, I. N. (2008) *Mol. Pharmacol.* **73,** 1203–1212
47. Hopkins, P. M. (2000) *Br. J. Anaesth.* **85,** 118–128
48. Allard, B., Couchoux, H., Pouvreau, S., and Jacquemond, V. (2006) *J. Physiol.* **575,** 69–81
49. Pan, Z., Yang, D., Nagaraj, R. Y., Nosek, T. A., Nishi, M., Takeshima, H., Cheng, H., and Ma, J. (2002) *Nat. Cell Biol.* **4,** 379–383
50. Reichelt, S. and Amos, W. B. (2001) *Microsc. Anal.* **86,** 9–11